Picosecond IR−UV Pump−Probe Study on the Vibrational Relaxation of Phenol−Ethylene Hydrogen-Bonded Cluster: Difference of Relaxation Route/Rate between the Donor and the Acceptor Site Excitations

Yuji Yamada, Masakazu Kayano, and Naohiko Mikami

Department of Chemistry, Graduate School of Science, Tohoku University, Sendai 980-8578 Japan

Takayuki Ebata*

Department of Chemistry, Graduate School of Science, Hiroshima University, Higashi Hiroshima 1-3-1, 739-8526 Japan

Received: December 9, 2005; In Final Form: February 14, 2006

Picosecond time-resolved IR−UV pump−probe spectroscopy has been performed to study intracluster vibrational energy redistribution (ICVR) and vibrational predissociation (VP) for the OH and CH stretch vibrations of phenol−ethylene hydrogen-bonded cluster. The transient UV spectra after the picosecond IR pulse excitation of these modes were observed by 1+1 REMPI via S_1 with a picosecond UV pulse. We have focused on the difference of the energy flow routes and their rates between the donor (phenol) and the acceptor (ethylene) site. Though the transient UV spectra showed a similar broad feature for all the vibrations examined, the time profiles exhibited a remarkable site dependence, as well as substantial mode dependence. Especially, we found a large difference in the early stage of the IVR evolution and the rates, whereas the VP rates were very similar.

I. Introduction

The vibrational relaxation has been widely studied experimentally and theoretically because of its fundamental importance in chemistry.[1,2] In the condensed phase, a large number of studies have been reported on the intramolecular vibrational relaxation (IVR) and intermolecular vibrational energy transfer (VET) by using various time-resolved pump−probe techniques with ultrashort laser pulses.[3−13] According to these extensive works, it is widely established that the energy put into the high-frequency vibrational level such as OH and CH stretches is first redistributed within the molecule in a few picoseconds, and the energy is further redistributed into the surrounding molecules. In parallel, a large number of studies on the vibrational relaxation have been reported for gas-phase molecules and clusters.[3,14−21] A major target of the studies on molecular clusters is to elucidate precisely the energy dissipation routes and obtain each rate constant from the knowledge of the anharmonic coupling, the density of states of bath mode, and the relative orientation between solute and solvent molecules. Among many works, we have been studying the dynamics of the X−H stretching vibration, where X refers to O, C, or N atom, of isolated molecules as well as their clusters in S_0 by means of picosecond IR−UV pump−probe spectroscopy.[22−26]

In previous papers, we reported the vibrational relaxation of the OH and NH_2 stretching vibration of phenol and aniline respectively, in supersonic beams.[24,26] For phenol we also reported the relaxation of the OH stretching vibration of hydrogen-bonded (H-bonded) clusters.[24] In that work, we found that the energy dissipation started from the high-frequency OH stretching vibration proceeds by three steps: (1) first, IVR within the phenolic site, (2) second, the energy dissipation into the whole cluster, and (3) finally, the vibrational predissociation (VP) of the H-bond. Among the three steps, it was found that the H-bond considerably accelerates the first step. Our observation strongly indicated that the relaxation route in a gas phase is very similar to that in a condensed phase.

In the present work, we report a further study on the IVR/VP of phenol−ethylene H-bonded cluster by the real time observation. The phenol−ethylene cluster is known to be bound by π-type H-bond between phenolic OH and the π-electrons of the ethylene.[27] We reported the relaxation of the H-bonded OH stretching vibration of this cluster in our previous paper,[24] and in this report we concentrate on the relaxation of the CH stretching vibrations. In the phenol−ethylene cluster, there are two types of the CH stretching vibrations; the CH stretches of the phenolic site (H-donor site) and those of the ethylene site (H-acceptor site). Though the frequencies of these vibrations (3000−3100 cm^{-1}) are not so different from each other, their relaxation mechanism and rate constants will be quite different because of the different character of the modes and as well as the site. We will discuss the dynamics of the relaxation of these high-frequency vibrations, by combing the results of the OH stretch vibration reported in our previous paper.[24]

II. Experiment

A detailed description of the experimental setup of picosecond IR−UV pump−probe spectroscopy was given in our previous papers.[22] Briefly, a fundamental output (1.064 μm) of a mode-locked picosecond Nd^{3+}:YAG laser (Ekspra PL2143B) was split into two parts. The major one was frequency tripled and was introduced into an OPG/OPA and SHG system (Ekspra PG401SH) for a tunable UV light generation. For the generation of tunable IR light pulse, the minor part of the 1.064 μm output was introduced into a homemade OPG/OPA system consisting of a pair of $LiNbO_3$ crystals. Two crystals were separated by 1 m and placed on rotational stages. The spectral resolution of

10.1021/jp0571832 CCC: $33.50
Published on Web 04/21/2006

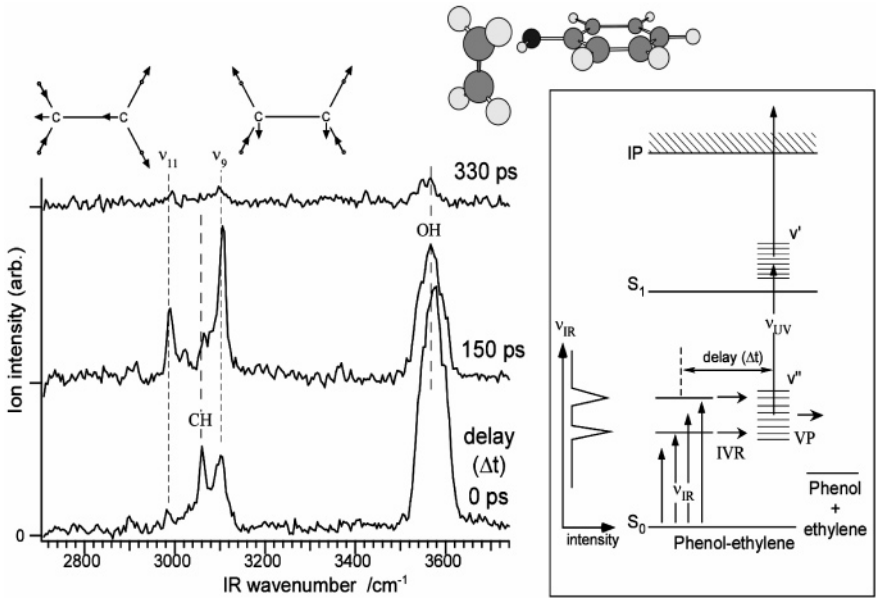

Figure 1. Ion-gain IR spectra of phenol−ethylene in a supersonic beam at several time delays. The probe UV frequency is fixed at 35 820 cm^{-1}. The inset describes the energy diagram and the excitation scheme of the ion-gain measurement.

the tunable UV light was 7 cm^{-1}, whereas that of the IR light was 15−20 cm^{-1} depending on the wavelength. The temporal shapes of the pump and probe laser pulses were determined by fitting the time profile of the cross correlation of the ammonia ionization, which was well reproduced by assuming a Gaussian shape for both the two pulses having fwhm of 12 ps.[28]

The jet-cooled phenol−ethylene cluster was generated by a supersonic expansion of phenol vapor seeded in ethylene (2%)/He mixed carrier gas at a total pressure of 3 bar into vacuum through a pulsed nozzle (General valve) having a 0.8 mm aperture. The free jet was skimmed by a skimmer with a 0.8 mm diameter aperture (Beam dynamics) located at 30 mm down stream of the nozzle. The IR and UV lasers were introduced into a vacuum chamber in a counterpropagated manner and crossed the supersonic beam at 50 mm down stream of the skimmer. The molecules in the supersonic beam were ionized by 1+1 resonance enhanced multiphoton ionization (REMPI) via the S_1 state, and the ions were repelled to the direction perpendicular to the plane of the molecular beam and the laser beams. The ions were then mass-analyzed by a 50 cm time-of-flight tube and were detected by an electron multiplier (Murata Ceratron). The transient profiles of the pump−probe ion signals were observed by changing a delay time between UV and IR pulses by a computer controlled optical delay line.

Phenol (99.0%) was purchased from Wako Chemicals Industry Ltd. and was purified by vacuum distillation before use. Ethylene was purchased from Nippon Sanso.

III. Results and Discussion

A. IR Spectrum of Phenol−Ethylene Cluster. Figure 1 shows the ion-gain IR spectra of phenol−ethylene H-bonded cluster. An excitation scheme is shown in the inset. In the figure, three IR spectra obtained at different delay times (0, 150 and 330 ps) between the IR and the UV laser pulses are shown. The UV laser frequency (ν_{UV}) was fixed at 35820 cm^{-1} in all the spectra, which refers to the transitions ($\upsilon'-\upsilon''$) from the IVR redistributed levels (υ'') after the IR pulse excitation. In Figure 1, an intense peak at 3580 cm^{-1} is the H-bonded phenolic OH stretching vibration, and three bands at 2987, 3054, and 3104 cm^{-1} are assigned to mode 11 (ν_{11}) of ethylene, phenolic CH stretch, and mode 9 (ν_9) of ethylene, respectively.[29] In ethylene, it was reported that ν_{11} with b_{3u} symmetry is coupled with $\nu_2 + \nu_{12}$ and $2\nu_{10} + \nu_{12}$ combination bands by anharmonic resonance.[30−32] However, the split between ν_{11} and the combination bands is as large as 100 cm^{-1}, which is larger than the spectral resolution of the present IR laser pulse. We assume a similar split is held in the cluster so that the picosecond IR pulse can excite only this band. As seen in the spectra, the relative intensity of the IR bands is quite different at different delay times. For example, the ion intensities are intense at $\Delta t \sim 0$ ps for both the H-bonded OH and the aromatic CH stretches in phenolic site and decrease gradually with the time. On the other hand, there is a significant delay for the electronic transition to be maximum for the ethylene CH stretches, such as ν_{11}. Because the UV transition reflects the population of the IVR redistributed levels (υ''), we conclude that there is a large difference in the energy randomization time scale for the CH stretch at different site. At longer delay times, all the bands disappear owing to VP of the H-bond.

B. Transient UV Spectra and Time Evolutions of IVR Redistributed Levels. Figure 2 shows the transient UV spectra observed after the excitations of the (a) phenolic OH stretch and the (b) ethylene CH stretch (ν_9). In case of the phenolic OH stretch vibration, Figure 2a, the transient UV spectrum exhibits a broad feature extending down to 34 000 cm^{-1} at short delay times. The broad feature indicates these transitions are assigned to that of the IVR redistributed levels. As seen in the figure, at the delay time of 90 ps, the ion signals at frequencies lower than ~35 000 cm^{-1} disappear, whereas the ion intensity at higher frequency region remains at longer delay times. At a delay time of 400 ps, almost all the ion signals disappear due to the vibrational predissociation (VP). A similar feature was observed in the transient UV spectrum for the IR excitation of the phenolic CH stretch vibration (not shown). On the other hand, in the case of the ethylene CH stretch (ν_9) excitation, Figure 2b, the broad UV transition appears in the region above ~35 000 cm^{-1}, and the intensity decays uniformly in all the UV region.

We then measured the time profiles of the broad UV transition at several UV frequencies after exciting the OH and the CH stretch vibrations, which are shown as the dotted curves in Figure 3. There are two prominent features: First, the time

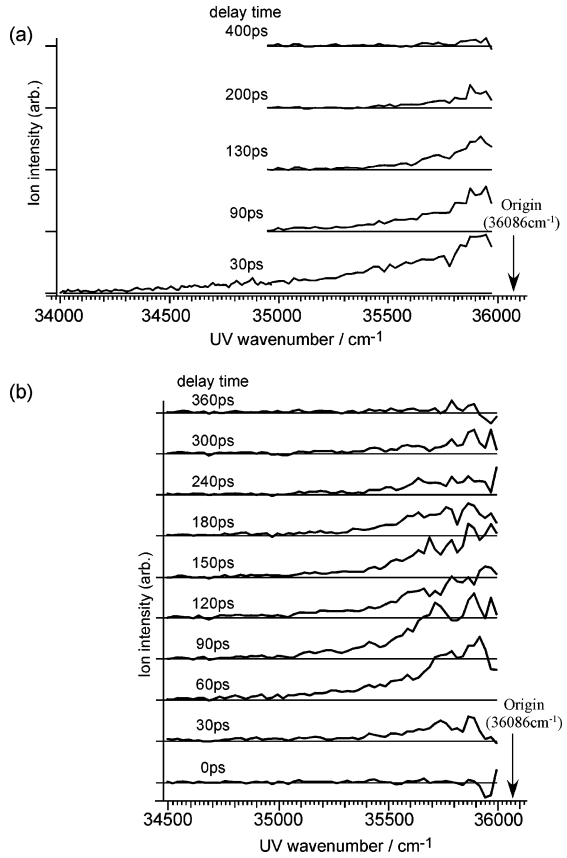

Figure 2. Transient 1+1 REMPI spectra of the phenol−ethylene cluster obtained at several delay times after IR pumping of the (a) phenolic OH stretch and (b) mode 9 of ethylene sites.

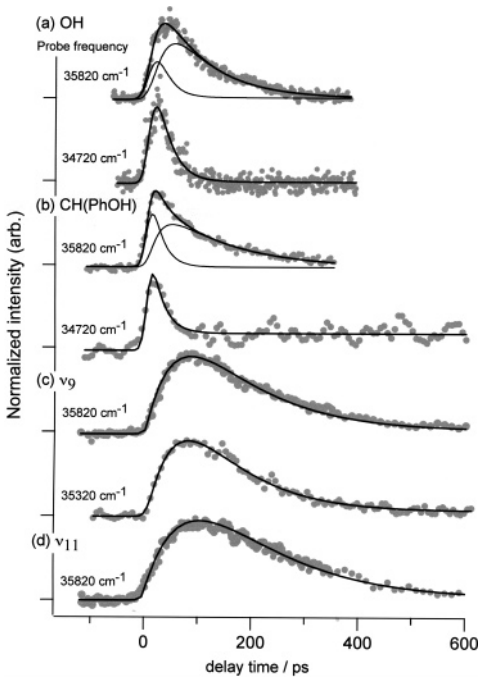

Figure 3. Time evolutions of the transient UV signals after IR pumping (a) the phenolic OH stretching vibration at 3580 cm^{-1}, (b) phenolic CH stretches at 3054, (b) ethylene CH mode 9 at 3104 cm^{-1}, and (d) mode 11 of ethylene CH stretches at 2987 cm^{-1}. The numbers in the figure are the frequencies of the probe UV laser. The solid curves are convoluted ones using two types of relaxation models, and thin curves in (a) and (b) indicate the components from "hot phenol" and "hot cluster", respectively (see text). The ratio, A/B, of the relative components is (a) (upper trace) A/B = 1.15, (lower trace) A/B = 0.0 and (b) (upper trace) A/B = 1.76, (lower trace) A/B = 0.0.

profiles are dependent on the monitoring UV frequencies for the phenolic OH and the CH stretching vibrations. For example, in case of phenolic CH stretch excitation (Figure 3b), the ion intensity reaches to the maximum at 18 ps and disappears at ~300 ps when UV is fixed to 35 820 cm^{-1}, whereas they change to 10 and 80 ps, respectively, when UV is fixed to 34 720 cm^{-1}. A similar feature is observed for the OH stretch excitation in Figure 3a, the intensities monitored at 35 820 cm^{-1} reach a maximum at 40 ps and disappear at 300 ps, whereas the intensity monitored at 35 820 cm^{-1} reaches a maximum at 20 ps and disappears at ~80 ps. On the other hand, the time profiles of the ion signals after the ethylene CH stretch are almost independent of the monitoring UV frequencies. In addition, the times of the ion intensity to reach to the maximum are slower in the ethylene CH excitation than in the phenolic CH excitation. As seen in Figure 3c, the profiles observed at 35 820 and 35 320 cm^{-1} are almost identical for the ν_9 excitation of the ethylene site; that is, they reach the maxima at 95 ps and disappear at ~600 ps. These time profiles are in accordance with the feature of the transient UV spectra shown in Figure 2. That is, in the phenolic OH excitation, the ion intensity at a frequency lower than 35 000 cm^{-1} disappears faster than that at a higher frequency, whereas in the ν_9 excitation the ion intensity disappears uniformly at all the UV frequencies.

As was reported in our previous paper, we stated that, in the broad transient UV spectra, the transitions in the region lower than 35 000 cm^{-1} mainly consist of the hot band transitions of phenolic site, that is, "hot phenol transition", whereas the transitions appearing in the higher frequency region are assigned to those of the internally excited cluster, "hot cluster" transition. There are two reasons why we assigned the lower frequency part (ν_{UV} < 35 000 cm^{-1}) to that of "the hot phenol transition" and the higher frequency part to the "hot cluster transition". First, the ion intensity in the lower frequency region disappears faster than that in the higher frequency region. Second, in general, the vibrational frequencies of intermolecular modes are lower than 150 cm^{-1}, so that the largely red-shifted transitions, more than 1000 cm^{-1} red-shifted from the cluster 0,0 band, are hardly attributed to the hot band transitions of intermolecular modes due to the unfavorable Franck−Condon activity. Thus, we concluded the following energy dissipation pathway starting from the OH stretching vibration,

$$\mathrm{Ph(OH)^*{-}C_2H_4 \rightarrow (PhOH)^*{-}C_2H_4 \rightarrow (PhOH{-}C_2H_4)^* \rightarrow PhOH + C_2H_4} \quad (1)$$

where Ph(OH)*, (PhOH)* and (PhOH−C_2H_4)* are the IR excited phenol, hot phenol, and hot cluster, respectively. This three-step relaxation model was described in our previous paper; the energy of the IR pumped level is first redistributed into the vibrational modes of the phenolic site ($IVR_{molecular}$, τ_1) forming hot phenol, (PhOH)*.[24] The energy is further randomized into the vibrations of the whole cluster ($IVR_{cluster}$, τ_2) forming a hot cluster, (PhOH−C_2H_4)*. Finally, the H-bond is dissociated with a lifetime of τ_3. Because the time profile of the phenolic CH stretching vibration shows a feature similar to that of the phenolic OH, a similar energy flow scheme can be applied to the relaxation of this vibration. The time profiles of (PhOH)*−C_2H_4 and (PhOH−C_2H_4)* are expressed by the following equations,

$$I_{\mathrm{intramolecule}}(t) = I_0 \frac{\tau_2}{\tau_2 - \tau_1}(e^{-t/\tau_2} - e^{-t/\tau_1}) \quad (2a)$$

and

$$I_{\text{intracluster}}(t) = I_0 \frac{\tau_1\tau_2{\tau_3}^2}{(\tau_2-\tau_1)(\tau_3-\tau_2)(\tau_3-\tau_1)} \times \left\{\left(\frac{1}{\tau_2}-\frac{1}{\tau_3}\right)e^{-t/\tau_1} - \left(\frac{1}{\tau_1}-\frac{1}{\tau_3}\right)e^{-t/\tau_2} + \left(\frac{1}{\tau_1}-\frac{1}{\tau_2}\right)e^{-t/\tau_3}\right\} \quad (2b)$$

Though the electronic transition of (PhOH)*−C_2H_4 is located mainly below 35 000 cm^{-1} and that of (PhOH−C_2H_4)* is above 35 000 cm^{-1}, they are overlapped so that the observed time profile is expressed by the sum of eqs 2a and 2b. Thus, the observed time profile is expressed as

$$I(t) = A(\nu_{UV})\, I_{\text{intramolecule}}(t) + B(\nu_{UV})\, I_{\text{intracluster}}(t) \quad (3)$$

where $A(\nu_{UV})$ and $B(\nu_{UV})$ are the coefficients that depend on the UV frequency. The time evolutions of these two components are shown as thin curves in Figures 3a,b. One notes that the time profile observed at 34 720 cm^{-1} shows only one component, namely "hot phenol", which provides us the decay lifetime of $IVR_{molecular}$. Another noticeable point is that in Figure 3b one sees that the curve monitored at 34 720 cm^{-1} does not reach to zero at the longer delay time, which is due to the unavoidable fragmentation from higher clusters. We reproduced this nonzero baseline by a step function by assuming that the fragmentation of higher clusters is very fast. The rate constants obtained by using this model are listed in Table 1.

Different from the vibrational relaxation started from the phenolic site, we did not observe the UV frequency dependence of the time profiles after the excitation of the ethylene site. Thus, we employed a simpler two-step model; that is, the energy put into the CH stretch mode is redistributed within whole the cluster with a lifetime of τ_1, forming (PhOH−C_2H_4)*, which is followed by the dissociation with a lifetime of τ_2.

$$\text{PhOH}-(C_2H_4)^* \rightarrow (\text{PhOH}-C_2H_4)^* \rightarrow \text{PhOH} + C_2H_4 \quad (4)$$

The time profile of the hot cluster transition is expressed by

$$I(t) = I_0 \frac{\tau_2}{\tau_2-\tau_1}(e^{-t/\tau_2} - e^{-t/\tau_1}) \quad (5)$$

The time profile obtained in this model is independent of the UV frequency and the simulated curves well reproduce the observed time profiles as shown by solid curves in Figure 3. The validity of using this model will be discussed later. The observed time constants obtained on the basis of this model are also listed in Table 1. It should be commented that in Table 1 it is possible to give the opposite assignment of the obtained time constants to $\tau(IVR_{cluster})$ and $\tau(VP)$ of the CH stretch vibrations, because in eq 5 we obtain the same curve even if τ_1 and τ_2 are exchanged. The reason we assigned the shorter lifetimes to $\tau(IVR_{cluster})$ is that it is very unlikely that the $\tau(VP)$ from the CH stretch is faster than that from the OH stretch (90 ps).

C. Comparison of the Relaxation Rates and Mechanism between the Two Sites. Before discussing the rate constants listed in Table 1, we first discuss the site dependence of the IVR process; the three-step process from the phenolic site and two-step process from the ethylene site. This difference is explained by the fact that intramolecular vibrational energy redistribution (IMVR) is very fast in bare phenol, whereas it is very slow in bare ethylene. As was shown in previous paper, in bare phenol the IVR rate constants of the OH and the CH stretch is as fast as 14 and 5 ps, respectively, which was attributed to the energy flow into the strongly coupled levels ("the doorway sates") within the molecule.[23] Thus, even in the cluster the first energy dissipation process from the phenolic site will be IMVR within the phenolic site, which is followed by the energy flow into the intermolecular vibrational mode, that is, intracluster vibrational energy redistribution (ICVR), and the dissociation of H-bond.

Different from phenol, the vibrational levels at the CH stretch of ethylene are sparse because of the lower number of vibrational modes (12) than that of phenol (33), and even the lowest frequency mode has a high frequency as large as 826 cm^{-1}.[32] Thus, IVR will occur only in the cluster, and the vibrational energy put into the ethylene site mostly flows into the intermolecular mode, that is, ICVR. It also implies that the order of the anharmonic coupling in this process is high, resulting in slow ICVR, as seen in Table 1; that is, $\tau(IVR_{cluster})$'s in the ethylene site (62 and 100 ps) are slower than those in the phenolic site (20 ps). Then, this fast $IVR_{cluster}$ of the phenolic site is attributed to the lower order coupling between the low-frequency intramolecular vibrations of "hot phenol" and the bath modes consisting of intermolecular modes. Such low-frequency intramolecular vibrations are called "gateway mode"[7] or "doorway vibration"[33] in a condensed phase, and the energy transfer from the "gateway state" to solvents is considered to be very fast.[34]

The vibrational dynamics at the CH stretch level of the ethylene clusters, such as the ethylene dimer and nitrous oxide−ethylene dimer, has been investigated by Miller and coworkers.[35,36] In these clusters, only VP but no IVR occurs, indicating the stronger "CH stretch ↔ dissociation continuum" coupling than the "CH stretch ↔ bath states anharmonic" coupling. However, in the present study it was found that in phenol−ethylene the initial step from the ethylene CH stretch is IVR within the cluster, which means stronger "CH stretch ↔ bath states" anharmonic coupling than "CH stretch ↔ dissociation continuum" coupling in this cluster. This result indicates that the bath states consist of not only the intermolecular modes but also the vibrational levels belonging to the phenolic site. Thus, the energy deposit into the ethylene CH stretch will be immediately dissipated to the whole cluster via the vibrational

TABLE 1: Obtained Time Constants (ps) of Intramolecular Vibrational Energy Redistribution ($IVR_{molecular}$), Intracluster Vibrational Energy Redistribution ($IVR_{cluster}$) and Vibrational Predissociation (VP) of the Phenol−Ethylene Cluster

mode	frequency (cm^{-1})	$IVR_{molecular}$ (ps)	$IVR_{cluster}$ (ps)	VP (ps)	$(k_{diss})^{-1}$ (ps) $D_0 = 900\ cm^{-1}$	$D_0 = 1000\ cm^{-1}$	$D_0 = 1100\ cm^{-1}$
phenol OH[a]	3580	10 ± 2	20 ± 4	90 ± 10	2.0	3.1	4.6
ethylene mode 9	3104	*b*	62 ± 8	100 ± 10	3.1	4.8	7.5
phenol CH	3054	≤5	20 ± 3	120 ± 20	3.2	5.0	7.8
ethylene mode 11	2987	*b*	100 ± 10	110 ± 20	3.3	5.3	9.1

[a] Kayano et al.[24] [b] In the cases of the ethylene CH stretch excitations, intramolecular relaxation to ethylene modes was not observed, but the direct intracluster relaxation to the whole cluster in the first relaxation step. See text.

TABLE 2: Vibrational Frequencies of Intermolecular Mode of Phenol−Ethylene Hydrogen-Bonded Cluster Obtained by MP2/6-31G* Level ab Initio Calculation

Frequency (cm^{-1})	mode
15.0	torsion
21.3	out-of plane bend
33.1	in-plane bend
78.2	out-of plane wagging
91.4	in-plane wagging
119.0	stretch

levels belonging to the phenolic site as well as the intermolecular vibrational levels.

D. Estimation of Predissociation Rates with RRKM Theory. Another point noticed in Table 1 is that the VP lifetimes are not so different for different vibrations as well as the sites. For the CH stretching vibrations, the similarity of the VP rate constants can be understood if we assume that VP occurs after the complete energy randomization within the cluster, because their vibrational frequencies are not so different from each other. In this sense, it is suggested that the rate constants can be compared with those predicted by the statistical model, such as RRKM calculation.[37] On the other hand, a similar VP rate constant was obtained for the OH stretch, 90 ps. The OH stretch frequency is 400−500 cm^{-1} higher than that of the CH stretch, so that we expect a much faster VP than those of the CH stretches if we assume statistical model. So, we calculated the $k_{diss}(E)$ for phenol−ethylene cluster at 3000 and 3580 cm^{-1}. In RRKM theory, the dissociation rate constant at the total energy of E is expressed as

$$k_{diss}(E) = G^{\ddagger}(E - D_0)/h\rho(E) \quad (6)$$

Here $G^{\ddagger}(E - D_0)$ is the number of possible states of fragments at an available energy of $E - D_0$, and $\rho(E)$ is the density of states of the clusters. For the estimation of vibrational density of states, we first obtained the optimized structure of the cluster and the vibrational frequencies by ab initio calculation with the MP2/6-31G* level in Gaussian 98 package.[38] For the vibrations of phenolic sites we multiplied a scaling factor of 0.96 to reproduce the H-bonded OH frequency,[27] and we used literature values for the vibrations of ethylene.[32] In Table 2, the calculated vibrational frequencies of the intermolecular modes are listed. These frequencies were used without multiplying a scaling factor. The density of states calculation was carried out by the direct counting method without considering the vibrational anharmonicity because of the difficulty of its estimation. This neglect will overestimate the $k_{diss}(E)$ value. For the binding energy of the π−type H-bond, we do not have a reliable value. The high-level calculation for the water−ethylene π−type H-bond energy was reported to be 2.27 kcal/mol.[39] Because phenol is slightly more acidic ($pK_a = 9.9$) than water, the binding energy of the phenol−ethylene H-bond may be larger than that of water−ethylene. So, we estimated the binding energy to be in the range 900−1100 cm^{-1} (2.6−3.1 kcal/mol). The dissociation lifetimes, $[k_{diss}(E)]^{-1}$, calculated as a function of dissociation energy are also shown in Table 1. As seen in the table, the calculated rate constants are 30−45 times larger than those observed. The discrepancy may be partly due to the fact that we neglected the vibrational anharmonicity in the calculation, and/or the dissociation does not take place after the completed randomization. As to the trend of the increase of the rate with the energy, the RRKM exhibits qualitative agreement. That is, the observed rate constant at the OH stretch is about 1.2 times larger than that at the CH stretch, whereas it is about 1.6−1.7 in the RRKM calculation, which is not so sensitive to the examined binding energy. At this moment, it is difficult to conclude the validity of RRKM prediction to the dynamics of phenol−ethylene, and it is necessary to perform this investigation in wider energy region.

IV. Conclusion

In this article, a picosecond time-resolved IR−UV pump−probe spectroscopy has revealed the relaxation mechanism of the OH and CH stretching vibrations of the jet-cooled phenol−ethylene cluster in the S_0 state. The phenolic OH and CH stretching vibrations showed very rapid energy flow into the phenolic bath mode (10 ps in OH and ≤5 ps in CH stretch), followed by a further dissipation into the whole cluster. On the other hand, the energy of the ethylene CH stretching vibrations, ν_9 and ν_{11}, directly flows into the whole cluster. These two types of pathways are attributed to the existence of the strongly coupled bath modes in the phenolic site but not in the ethylene site. In contrast, the time constants of VP were not so different among the examined modes, that is, 90 ps for the OH and 100−120 ps for the CH stretch. Though the results suggested a complete energy randomization before VP, the RRKM calculation did not give a satisfactory agreement with respect to the absolute values.

Acknowledgment. We acknowledge Profs. A. Fujii, H. Ishikawa, and Dr. T. Maeyama for their helpful discussion. This work is supported by Grant-in-Aids for Scientific Research (No. 1535002) by JSPS. Y.Y. is thankful for the support from COE project of Tohoku University. N.M. acknowledges the support for Grant-in-Aids for specially Promoted Research (No. 16002006) by MEXT.

References and Notes

(1) Nesbitt, D. J.; Field, R. W. *J. Phys. Chem.* **1996**, *100*, 12735.
(2) Owrutsky, J. C.; Raftery, D.; Hochstrasser, R. M. *Annu. Rev. Phys. Chem.* **1994**, *45*, 519.
(3) Yoo, H. S.; McWhorter, D. A.; Pate, B. H. *J. Phys. Chem. A* **2004**, *108*, 1380.
(4) Lock, A. J.; Bakker, H. J. *J. Chem. Phys.* **2002**, *117*, 1708.
(5) von Benten, R.; Link, O.; Abel, B.; Schwarzer, D. *J. Phys. Chem. A* **2004**, *108*, 363.
(6) Assmann, J.; von Benten, R.; Charvat, A.; Abel, B. *J. Phys. Chem. A* **2003**, *107*, 1904.
(7) Cheatum, C. M.; Heckscher, M. M.; Bingemann, D.; Crim, F. F. *J. Chem. Phys.* **2001**, *115*, 7086.
(8) Heckscher, M. M.; Sheps, L.; Bingemann, D.; Crim, F. F. *J. Chem. Phys.* **2002**, *117*, 8917.
(9) Elles, C. G.; Cox, M. J.; Crim, F. F. *J. Chem. Phys.* **2004**, *120*, 6973.
(10) Wang, Z.; Pakoulev, A.; Pang, Y.; Dlott, D. D. *J. Phys. Chem. A* **2004**, *108*, 9054.
(11) Vierheiling, A.; Chen, T.; Waltner, P.; Kiefer, W.; Materny, A.; Zewail, A. H. *Chem. Phys. Lett.* **1999**, *312*, 349.
(12) Asbury, J. B.; Steinel, T.; Stromberg, C.; Gaffney, K. J.; Piletic, I. R.; Goun, A.; Fayer, M. D. *Phys. Rev. Lett.* **2003**, *91*, 237402.
(13) Banno, M.; Sato, S.; Iwata, K.; Hamaguchi, H. *Chem. Phys. Lett.* **2005**, *412*, 464.
(14) Felker, P. M.; Zewail, A. H. *J. Chem. Phys.* **1985**, *82*, 2975.
(15) Callegari, A.; Merker, U.; Engles, P.; Srivastava, H. K.; Lehmann, K. K. Scoles, G. *J. Chem. Phys.* **2000**, *113*, 10583.
(16) Ebata, T.; Kayano, M.; Sato, S.; Mikami, N. *J. Phys. Chem. A* **2001**, *105*, 8623.
(17) Stromberg, C.; Meyers, D. J.; Fayer, M. D. *J. Chem. Phys.* **2002**, *116*, 3540.
(18) Meyers, D. J.; Shigeiwa, M.; Fayer, M. D.; Silbey, R. *Chem. Phys. Lett.* **1999**, *312*, 399.
(19) Lock, A. J.; Bakker, H. J. *J. Chem. Phys.* **2002**, *117*, 1708.
(20) Satink, R. G.; Bakker, J. M.; Meijer, G.; von Helden, G. *Chem. Phys. Lett.* **2002**, *359*, 163.
(21) Sampson, R. K.; Lawrance, W. D. *Chem. Phys. Lett.* **2005**, *401*, 440.

(22) Ebata, T.; Kayano, M.; Sato, S.; Mikami, N. *J. Phys. Chem. A* **2001**, *105*, 8623.
(23) Yamada, Y.; Ebata, T.; Kayano, M.; Mikami, N. *J. Chem. Phys.* **2004**, *120*, 7400.
(24) Kayano, M.; Ebata, T.; Yamada, Y.; Mikami, N. *J. Chem. Phys.* **2004**, *120*, 7410.
(25) Yamada, Y.; Mikami, N.; Ebata, T. *J. Chem. Phys.* **2004**, *121*, 11530.
(26) Yamada, Y.; Okano, J.-I.; Mikami, N.; Ebata, T. *J. Chem. Phys.* **2005**, *123*, 124316.
(27) Fuji, A.; Ebata, T.; Mikami, M. *J. Phys. Chem. A* **2002**, *106*, 8554.
(28) David, O.; Dedonder-Lardeux, C.; Jouvet, C.; Kang, H.; Martrenchard, S.; Ebata, T.; Sobolewski, A. L. *J. Chem. Phys.* **2004**, *120*, 10101.
(29) Sartakov, B. G.; Oomens, J.; Reuss, J.; Fayt, A. *J. Mol. Spectrosc.* **1997**, *185*, 31.
(30) Foster, R. B.; Hills, G. W.; Jones, W. J. *Mol. Phys.* **1977**, *33*, 1589.
(31) Bach, M.; Georges, R.; Hepp, M.; Herman, M. *Chem. Phys. Lett.* **1998**, *294*, 533.
(32) Georges, R.; Bach, M.; Herman, M. *Mol. Phys.* **1999**, *97*, 279.
(33) Dlott, D. D.; Fayer, M. D. *J. Chem. Phys.* **1990**, *92*, 3798.
(34) Dlott, D. D. *Chem. Phys.* **2001**, *266*, 149.
(35) Chan, M. C.; Block, P. A.; Miller, R. E. *J. Chem. Phys.* **1995**, *102*, 3993.
(36) Bemish, R. J.; Rhee, W. M.; Pedersen, L. G.; Miller, R. E. *J. Chem. Phys.* **1996**, *102*, 4411.
(37) Schuatz, G. C.; Ranter, M. A. *Quantum Mechanics in Chemistry*; Prentice Hall: Englrwood Cliffs, NJ, 1993).
(38) Frisch, M. J.; Trucks, G. W.; Schlegel H. B.; et al. *Gaussian 98*, revision A.7; Gaussian, Inc.: Pittsburgh, PA, 1998.
(39) Vorobyov, I.; Yappert, M. C.; Dupre, D. B. *J. Phys. Chem. A* **2002**, *106*, 10691.